

Generalized Fluid System Simulation Program (GFSSP), Version 6

Alok K. Majumdar,¹ Andre C. LeClair,² and Ric Moore³
NASA Marshall Space Flight Center, Huntsville, AL, 35824

and

Paul A. Schallhorn⁴
NASA Kennedy Space Center, FL, 32899

The Generalized Fluid System Simulation Program is a finite volume-based, general purpose computer program for analyzing steady state and time-dependent flow rates, pressures, temperatures, and concentrations in a complex flow network. The program is capable of modeling real fluids with phase changes, compressibility, mixture thermodynamics, conjugate heat transfer between solid and fluid, fluid transients, pumps, compressors, flow control valves, and external body forces such as gravity and centrifugal. The thermofluid system to be analyzed is discretized into nodes, branches, and conductors. The scalar properties such as pressure, temperature, and concentrations are calculated at nodes. Mass flow rates and heat transfer rates are computed in branches and conductors. The graphical user interface allows users to build their models using the “point, drag, and click” method; the users can also run their models and post-process the results in the same environment. The integrated fluid library supplies thermodynamic and thermophysical properties of 36 fluids, and 24 different resistance/source options are provided for modeling momentum sources or sinks in the branches. Users can introduce new physics as well as nonlinear and time-dependent boundary conditions through User Subroutine.

Nomenclature

L_1	=	initial length of the water volume in the pipe
L_g	=	initial length of the air column in the pipe
L_T	=	total length
P_R	=	ratio of reservoir pressure to the initial pressure of the entrapped air
p_{atm}	=	initial pressure of the entrapped air
p_R	=	reservoir pressure
V	=	volume
V_{12}	=	volume of water in node 12
V_{air}	=	volume of entrapped air
V_{tot}	=	total volume
α_g	=	ratio of initial air column length to total pipe length

I. Introduction

THE need for a generalized computer program for thermofluid analysis in a flow network has been felt for a long time in aerospace industries. Designers of thermofluid systems often need to know pressures, temperatures, flow rates, concentrations, and heat transfer rates at different parts of a flow circuit for steady state or transient conditions. Such applications occur in propulsion systems for tank pressurization, internal flow analysis of rocket engine

¹ Aerospace Engineer, Thermal and Combustion Analysis Branch, ER43, AIAA Senior Member.

² Aerospace Engineer, Thermal and Combustion Analysis Branch, ER43.

³ Software Engineer, Thermal and Combustion Analysis Branch, ER43.

⁴ Chief, Environments and Launch Approval Branch, VAH30, AIAA Senior Member.

turbopumps, chilldown of cryogenic tanks and transfer lines, and many other applications of gas-liquid systems involving fluid transients and conjugate heat and mass transfer. Computer resource requirements to perform time-dependent, three-dimensional Navier-Stokes computational fluid dynamics (CFD) analysis of such systems are prohibitive and therefore are not practical. A possible recourse is to construct a fluid network consisting of a group of flow branches such as pipes and ducts that are joined together at a number of nodes. They can range from simple systems consisting of a few nodes and branches to very complex networks containing many flow branches simulating valves, orifices, bends, pumps, and turbines. In the analysis of existing or proposed networks, node pressures, temperatures, and concentrations at the system boundaries are usually known. The problem is to determine all internal nodal pressures, temperatures, concentrations, and branch flow rates. Such schemes are known as network flow analysis methods, and they use largely empirical information to model fluid friction and heat transfer.

The oldest method for systematically solving a problem consisting of steady flow in a pipe network is the Hardy Cross method.¹ The Hardy Cross method works well for hand calculation but experiences slow convergence for large circuits. The network analysis method has been widely used in thermal analysis codes (SINDA/G² and SINDA/FLUINT³) using an electric analog. The partial differential equation of heat conduction is discretized into finite difference form expressing temperature of a node in terms of temperatures of neighboring nodes and ambient nodes. The set of finite difference equations are solved to calculate temperature of the solid nodes and heat fluxes between the nodes. The Generalized Fluid System Simulation Program (GFSSP)⁴ uses a “pressure-based” finite volume method⁵ as the foundation of its numerical scheme.

This paper provides a brief overview of GFSSP’s network definition, data structure, mathematical formulation, thermodynamic property program, and program structure and describes additional capabilities of version 6. The paper also describes several validation and verification efforts.

II. GFSSP Overview

A. Network Definition

GFSSP constructs a fluid network using fluid and solid nodes. The fluid circuit is constructed with boundary nodes, internal nodes, and branches (Fig. 1), while the solid circuit is constructed with solid nodes, ambient nodes, and conductors. The solid and fluid nodes are connected with solid-fluid conductors. Users must specify conditions such as pressure, temperature, and concentration of species at the boundary nodes. These variables are calculated at the internal nodes by solving conservation equations of mass, energy, and species in conjunction with the thermodynamic equation of state. Each internal node is a control volume where there is inflow and outflow of mass, energy, and species at the boundaries of the control volume. The internal node also has resident mass, energy, and concentration. The momentum conservation equation is expressed in flow rates and is solved in branches. At the solid node, the energy conservation equation for solid is solved to compute temperature of the solid node. Figure 1 shows a schematic and GFSSP flow circuit of a counter flow heat exchanger. Hot nitrogen gas is flowing through a pipe, colder nitrogen is flowing counter to the hot stream in the annulus pipe, and heat transfer occurs through metal tubes. The problem considered is to calculate flow rates and temperature distributions in both streams.

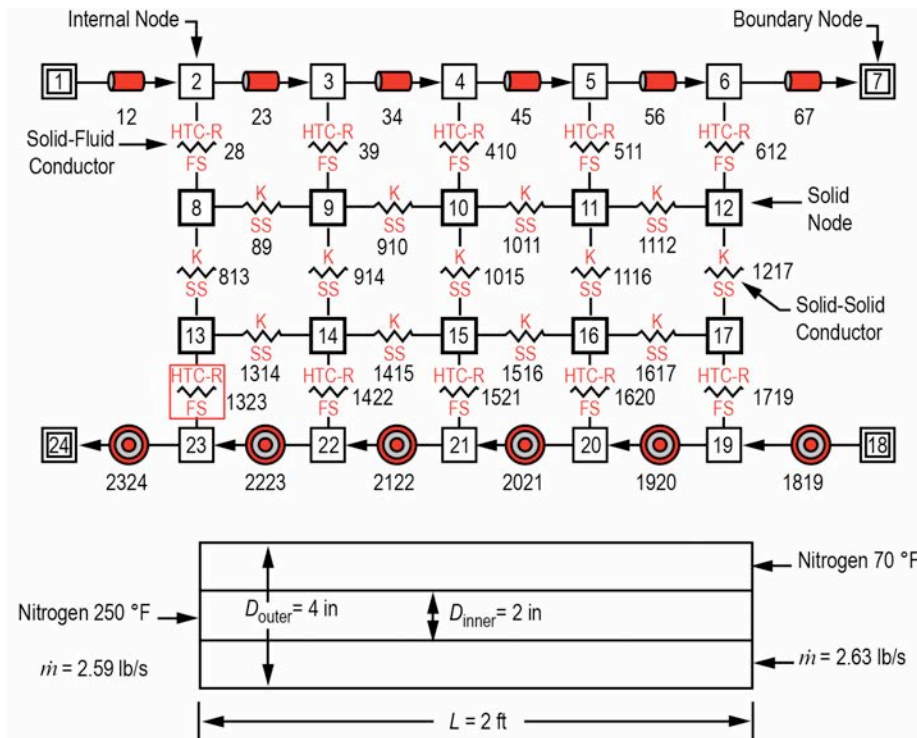


Figure 1. A typical flow network consists of a fluid node, solid node, flow branches, and conductors.

B. Data Structure

GFSSP has a unique data structure (Fig. 2) that allows constructing all possible arrangements of a flow network with no limit on the number of elements. The elements of a flow network are boundary nodes, internal nodes, and branches. For conjugate heat transfer problems, there are three additional elements: solid node, ambient node, and conductor. The relationship between a fluid node and a branch as well as a solid node and conductor is defined by a set of relational geometric properties. For example, the relational geometric properties of a node are the number and name of branches connected to it. With the help of these properties, it is possible to define any structure of the network as it progresses through every junction of the network. The positive or negative flow direction is also defined locally. Unlike a structured coordinate system, there is no global definition of flow direction and origin. The development of a flow network can start from any point and can proceed in any direction.

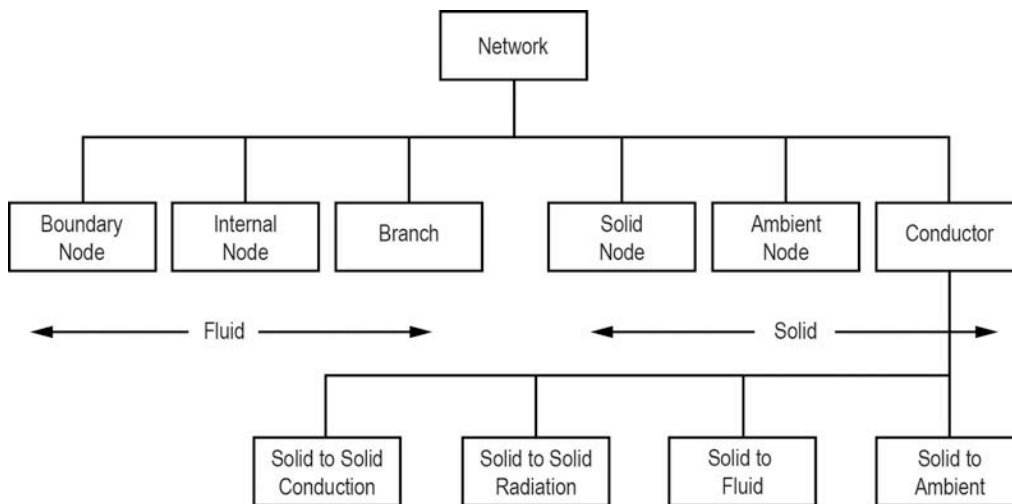


Figure 2. Data structure of the fluid-solid network has six major elements.

C. Mathematical Formulation

GFSSP solves the conservation equations of mass and momentum in internal nodes and branches to calculate fluid properties. It also solves for energy conservation equations to calculate temperatures of solid nodes. Table 1 shows the mathematical closure that describes the unknown variables and the available equations to solve the variables. Pressure, temperature, species concentration, and resident mass in a control volume are calculated at the internal nodes, whereas the flow rate is calculated at the branch. The equations are coupled and nonlinear; therefore, they are solved by an iterative numerical scheme. GFSSP employs a unique numerical scheme known as simultaneous adjustment with successive substitution (SASS), which is a combination of Newton-Raphson and successive substitution methods. The mass and momentum conservation equations and the equation of state are solved by the Newton-Raphson method, while the conservation of energy and species are solved by the successive substitution method.

Table 1. Mathematical closure.

Unknown Variables	Available Equations to Solve
Pressure	Mass conservation equation
Flow rate	Momentum conservation equation
Fluid temperature	Energy conservation equation of fluid
Solid temperature	Energy conservation equation of solid
Species concentrations	Conservation equations for species
Fluid mass (unsteady flow)	Thermodynamic equation of state

D. Fluid Properties

GFSSP is linked with two thermodynamic property programs, GASP⁶ and WASP⁷ and GASPAK,⁸ that provide thermodynamic and thermophysical properties of selected fluids. Both programs cover a range of pressure and temperature that allows fluid properties to be evaluated for liquid, liquid-vapor (saturation), and vapor region. GASP and WASP provide properties of 12 fluids (Table 2). GASPAK includes a library of 35 fluids (Table 3).

Table 2. Fluids available in GASP and WASP.

Index	Fluid	Index	Fluid
1	Helium	7	Argon
2	Methane	8	Carbon dioxide
3	Neon	9	Fluorine
4	Nitrogen	10	Hydrogen
5	Carbon monoxide	11	Water
6	Oxygen	12	RP-1

Table 3. Fluids available in GASPAK.

Index	Fluid	Index	Fluid
1	Helium	19	Krypton
2	Methane	20	Propane
3	Neon	21	Xenon
4	Nitrogen	22	R-11
5	Carbon monoxide	23	R-12
6	Oxygen	24	R-22
7	Argon	25	R-32
8	Carbon dioxide	26	R-123
9	Parahydrogen	27	R-124
10	Hydrogen	28	R-125
11	Water	29	R-134A
12	RP-1	30	R-152A
13	Isobutane	31	Nitrogen trifluoride
14	Butane	32	Ammonia
15	Deuterium	33	Ideal gas
16	Ethane	34	Hydrogen peroxide
17	Ethylene	35	Air
18	Hydrogen sulfide		

E. Program Structure

GFSSP has three major parts (Fig. 3). The first part is the graphical user interface, visual thermofluid analyzer of systems and components (VTASC). VTASC allows users to create a flow circuit by a “point and click” paradigm. It creates the GFSSP input file after the completion of the model building process. It can also create a customized GFSSP executable by compiling and linking User Subroutines with the solver module of the code. Users can run

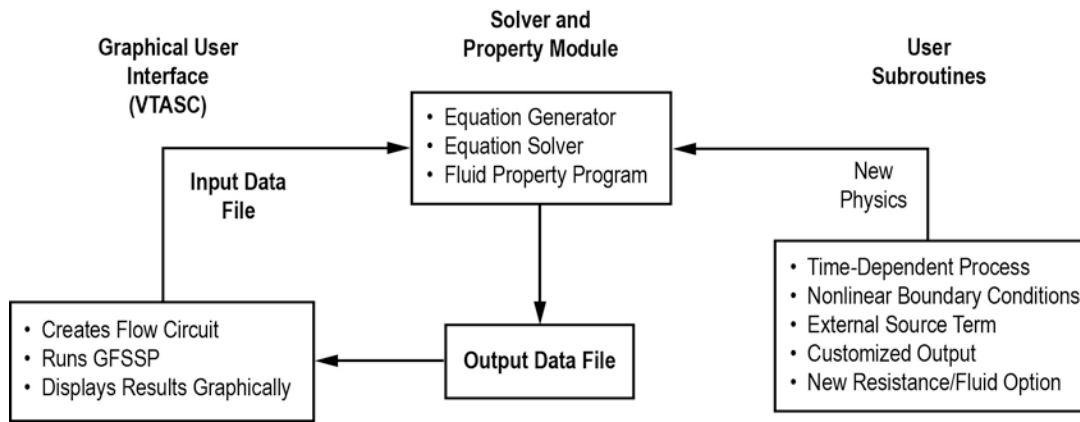


Figure 3. GFSSP's program structure showing the interaction of three major modules.

GFSSP from VTASC and post-process the results in the same environment. The second major part of the program is the solver and property module. This is the heart of the program that reads the input data file and generates the required conservation equations for all internal nodes and branches with the help of thermodynamic property data. It also interfaces with User Subroutines to receive any specific inputs from users. Finally, output files are created for VTASC to read and display results. The User Subroutine is the third major part of the program. This consists of several blank subroutines that are called by the Solver Module. These subroutines allow the users to incorporate any new physical model, resistance option, fluid, etc., in the model.

F. Resistance Option

In network flow analysis code, flow resistances are modeled after empirical laws. These empirical laws have been incorporated to model flow resistances for pipe flow, orifices, valves, and various pipe fittings. GFSSP models these flow resistances in the momentum conservation equation as a friction term. There are 24 different resistance options available for users to choose from. There is also a provision for introducing a new resistance option through User Subroutines. The available resistance options are shown in Table 4.

Table 4. Resistance options in GFSSP.

Option	Type of Resistance	Input Parameters	Option	Type of Resistance	Input Parameters
1	Pipe flow	L (in), D (in), ϵ/D	13	Common fittings and valves (two K method)	D (in), K_1 , K_2
2	Flow-through restriction	C_L , A (in ²)	14	Pump characteristics*	A_0 , B_0 , C_0 , A (in ²)
3	Noncircular duct	a (in), b (in)	15	Pump power	P (hp), η , A (in ²)
4	Pipe with entrance and exit loss	L (in), D (in), ϵ/D , K_e , K_e	16	Valve with given C_v	C_v , A
5	Thin, sharp orifice	D_1 (in), D_2 (in)	17	Joule-Thompson device	L_{Ω} , V_r , k_v , A
6	Thick orifice	L (in), D_1 (in), D_2 (in)	18	Control valve	See example 12 data file
7	Square reduction	D_1 (in), D_2 (in)	19	User defined	A (in ²)
8	Square expansion	D_1 (in), D_2 (in)	20	Heat exchanger core	A_f (in ²), A_s (in ²), A_c (in ²), L (in), K_c , K_e
9	Rotating annular duct	L (in), r_o (in), r_i (in), N (rpm)	21	Parallel tube	L (in), D (in), ϵ/D , n
10	Rotating radial duct	L (in), D (in), N (rpm)	22	Compressible orifice	C_L , A (in ²)
11	Labyrinth seal	r_i (in), c (in), m (in), n , α	23	Labyrinth seal, Egli correlation	r_i (in), c (in), m (in), n , α
12	Flow between parallel plates	r_i (in), c (in), L (in)	24	Fixed flow	Flow (lb _m /s), A (in ²)

* Pump characteristics are expressed as $\Delta p = A_0 + B_0 \dot{m} + C_0 \dot{m}^2$, Δp – Pressure rise, lbf/ft², \dot{m} – Flow rate, lbm/s.

G. Graphical User Interface

GFSSP's graphical user interface provides the users a platform to build and run their models. It also allows post-processing of results. The network flow circuit is first built using three basic elements: boundary node, internal node, and branch. Then, the properties of the individual elements are assigned. Users are also required to define global options of the model that include input/output files, fluid specification, and any special options such as rotation, heat exchanger, etc. During execution of the program, a run manager window opens up, and users can monitor the progress of the numerical solution. On the completion of the run, it allows users to visualize the results in tabular form for steady state solutions and in graphical form for unsteady solutions. It also provides an interface to activate and import data to the plotting program, Winplot,⁹ for post-processing.

H. Example Problems

Several example problems have been included to aid users to become familiar with different options of the code. The example problems also provide the verification and validation of the code by comparing code's predictions with analytical solution and experimental data. The examples include the following:

- 1) Simulation of a flow system consisting of a pump, valve, and pipeline.
- 2) Simulation of a water distribution network.
- 3) Simulation of compressible flow in a converging-diverging nozzle.
- 4) Simulation of the mixing of combustion gases and a cold gas stream.
- 5) Simulation of a flow system involving a heat exchanger.
- 6) Radial flow on a rotating radial disk.
- 7) Flow in a long-bearing squeeze film damper.
- 8) Simulation of the blowdown of a pressurized tank.
- 9) A reciprocating piston-cylinder.
- 10) Pressurization of a propellant tank.
- 11) Power balancing of a turbopump assembly.
- 12) Helium pressurization of liquid oxygen (LOX) and RP-1 propellant tanks.
- 13) Steady state and transient conduction through a circular rod, with convection.
- 14) Chillydown of a short cryogenic pipe line.
- 15) Simulation of fluid transient following sudden valve closure.
- 16) Simulation of pressure regulator downstream of a pressurized tank.
- 17) Simulation of flow regulator downstream of a pressurized tank.
- 18) Subsonic Fanno flow.
- 19) Subsonic Rayleigh flow.
- 20) Modeling of closed cycle liquid metal (lithium) loop with heat exchanger to heat helium gas.
- 21) Internal flow in a turbopump.
- 22) Simulation of a fluid network with fixed flow rate option.
- 23) Helium-assisted, buoyancy-driven flow in a vertical pipe carrying LOX with ambient heat leak.
- 24) Simulation of relief valve in a pressurized tank.
- 25) Two-dimensional recirculating flow in a driven cavity.
- 26) Fluid transients in pipes due to sudden opening of valve.
- 27) Boiling water reactor.
- 28) No-vent tank chill and fill model.
- 29) Self-pressurization of a cryogenic propellant tank due to boil-off.
- 30) Modeling solid propellant ballistic with GFSSP.

Tables 5a and 5b show the particular features of each example problem. For example, the Conjugate Heat Transfer option has been used in examples 13, 14, 23, 28, and 29.

Table 5a. Use of various options in example problems—examples 1–15.

Feature	Example														
	1	2	3	4	5	6	7	8	9	10	11	12	13	14	15
Conjugate heat transfer													13	14	
Constant property		2					7								
Cyclic boundary															
Fixed mass flow															
Flow regulator															
Gravity	1														
Heat exchanger					5						11				
Ideal gas								8							
Long inertia			3			6						12			
Fluid mixture				4						10		12			
Model import															
Moving boundary							7		9						
Multilayer insulation															
Multidimensional flow															
Noncircular duct							7								
Phase change														14	
Pressurization (tank)										10		12			
Pressure regulator															
Pressure relief valve															
Pump	1											12			
Solid rocket motor															
Turbopump											11				
Turbopump—internal flow															
Unsteady								8	9	10		12		14	15
User fluid															
User subroutine										10		12			
Valve O/C															15
Variable geometry									9						
Fluid transient (water hammer)															15

Table 5b. Use of various options in example problems—examples 16–30.

Feature	Example														
	16	17	18	19	20	21	22	23	24	25	26	27	28	29	30
Conjugate heat transfer								23					28	29	
Constant property										25					
Cyclic boundary					20										
Fixed mass flow							22						28		
Flow regulator		17													
Gravity								23				27	28	29	
Heat exchanger					20										
Ideal gas	16	17													30
Long inertia			18	19								27			30
Fluid mixture								23							
Model import								23							
Moving boundary											26*				
Multilayer insulation														29	
Multidimensional flow										25					
Noncircular duct															
Phase change												27	28	29	
Pressurization (tank)														29	
Pressure regulator	16														
Pressure relief valve									24						
Pump															
Solid rocket motor															30
Turbopump															
Turbopump—internal flow						21									
Unsteady	16	17					22	23	24		26		28	29	30
User fluid					20							27			
User subroutine			18	19	20						26		28	29	30
Valve O/C											26				
Variable geometry											26*				
Fluid transient (water hammer)											26				

*Variable geometry and moving boundary handled by User Subroutine.

III. Additional Capabilities of Version 6

The additional capabilities of version 6 include improved modeling of fluid mixtures, multidimensional flow capability in a system level flow network model, extension of the thermodynamic property package, extension of the pressure and flow regulator option, and inclusion of a relief valve and fixed flow rate options.

A. Mixture Modeling

The mixture modeling capability in the earlier version of GFSSP did not allow phase change for any component of the mixture. This limitation was due to the fact that the energy conservation equation was expressed as a product of specific heat and temperature instead of enthalpy. In many liquid propulsion applications, phase change in mixture is a common occurrence when cryogenic propellants mix with inert gas such as helium or nitrogen. This limitation was removed in version 6 by introducing an additional option where the energy equation of each species was expressed in terms of enthalpy. This option allows change of phase for any component of the mixture.

B. Multidimensional Flow Capability

Version 6 allows the user to model multidimensional flow in a fluid network. Network modeling usually applies to a system where a one-dimensional momentum equation is sufficient to characterize the flow. However, in some situations, such as a stratified cryogenic tank, the one-dimensional flow assumption is not realistic. Multidimensional flow modeling in a system level code will eliminate the need to integrate with a CFD code which has not yet been proved to be a practical solution. Multidimensional flow modeling in a system level code is a viable alternative to address such a need. Multidimensional capability in GFSSP has been verified by comparing its predictions with classical numerical fluid dynamics problems such as flow in a driven cavity.

C. Improvements and Extension in Thermodynamic Property Routines

There has been significant improvement and extension of the thermodynamic property routines in version 6. The thermodynamic property routines have been rewritten to introduce universal property call subroutines. In this process, the fluid property code has been reduced by nearly 1,000 lines. With the introduction of the new property call routines, User Subroutines can make property calls during any stage of the computation.

The user-supplied fluid property table has been extended to include an optional saturation table. It may be noted that earlier versions of GFSSP did not have the capability to model phase change with user-supplied fluid property tables. Utility programs have been developed to generate user-supplied thermodynamic property tables from tables generated by REFPROP¹⁰ and are included in the GFSSP installation package.

D. Extension of Pressure and Flow Regulator Option

A marching algorithm¹¹ for modeling pressure and flow regulator has been introduced in version 6. The earlier option of iterative algorithm is still available. The marching algorithm is more economic and allows the use of multiple regulators in a given flow circuit.

E. Inclusion of Relief Valve and Fixed Flow Rate Option

Version 6 has also the capability of modeling a relief valve and a fixed flow rate option. It may be recalled that GFSSP's mathematical formulation requires pressures to be specified at boundary nodes, and flow rates are calculated by solving the momentum conservation equation. In this version, the user can specify a given flow rate in a branch connected with a boundary node. This option is available for both steady and unsteady flow.

IV. Validation and Verification

Several code validation efforts were completed during the development of version 6. The applications considered for code validation include fluid transient, chilldown of cryogenic transfer line, self-pressurization of cryogenic tank, and no-vent chill and fill of cryogenic tank.

A. Two-Dimensional Recirculating Flow in a Square Cavity

In this example, two-dimensional recirculating flow in a square cavity¹² has been modeled using GFSSP's multidimensional flow calculation capability. In a square cavity, the flow is induced by shear interaction at the top wall, as shown in Fig. 4. The length of each wall is 12 in. The density of the fluid is assumed constant at $1 \text{ lb}_m/\text{ft}^3$, and the viscosity of the fluid is assumed to be $1 \text{ lb}_m/(\text{ft}\cdot\text{s})$. The bottom and side walls are fixed. The top wall is moving to the right at constant speed of 100 ft/s. The corresponding Reynolds number for this situation is $\text{Re} = 100$.

The GFSSP model (Fig. 5) of the driven cavity consists of 50 nodes (49 of which are internal) and 84 branches. The system model is shown in Fig. 5a. The expanded component (square cavity) is shown in Fig. 5b.

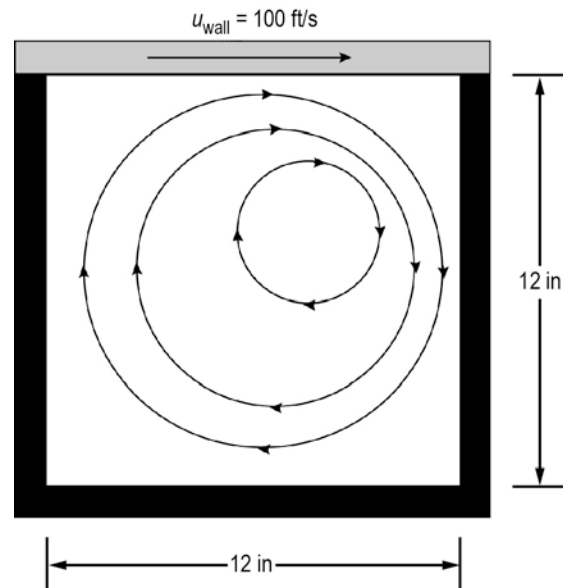


Figure 4. Flow in a shear driven square cavity.

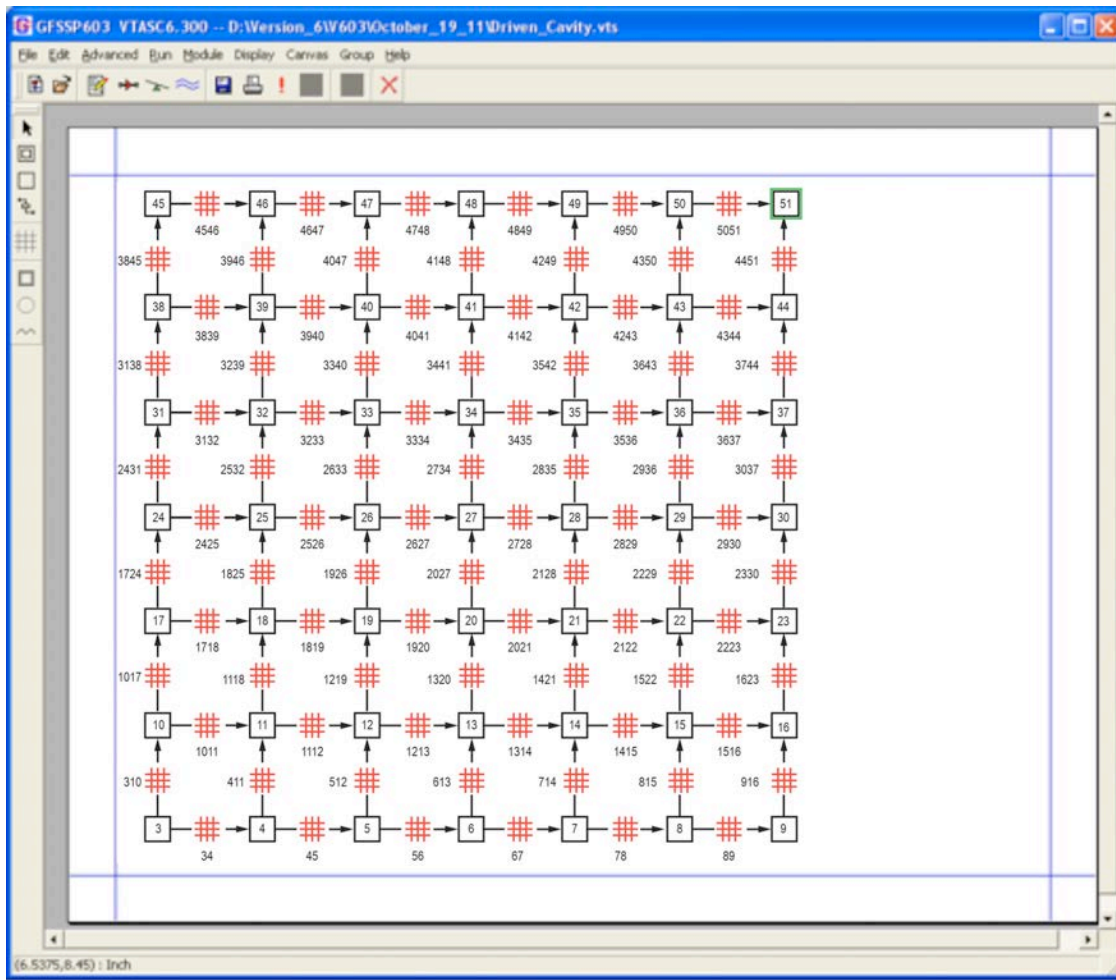
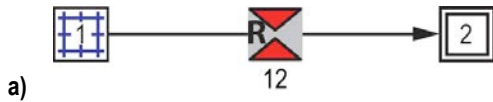


Figure 5. Two-dimensional Cartesian grid generation in VTASC: a) System network with expandable grid (element 1) and b) expanded two-dimensional Cartesian grid of element 1.

Figure 6 shows a comparison between the benchmark numerical solution and the GFSSP 7×7 node model velocity profiles along a vertical plane at the horizontal midpoint. As can be seen in Fig. 6, the results of this crude GFSSP model compare very favorably with the benchmark numerical solution of Burggraf.¹³

The predicted velocity field and pressure contours are shown in Fig. 7. The recirculating flow pattern and stagnation of flow near the top right corner are clearly shown in the figure. The predicted stream traces from the calculated velocity field are shown in Fig. 8.

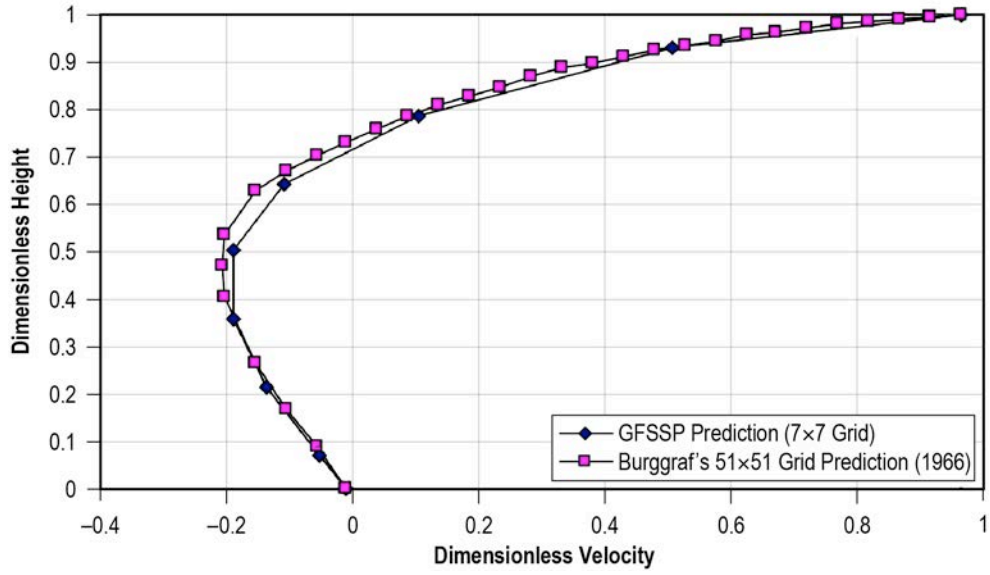


Figure 6. Shear driven square cavity centerline velocity distribution.

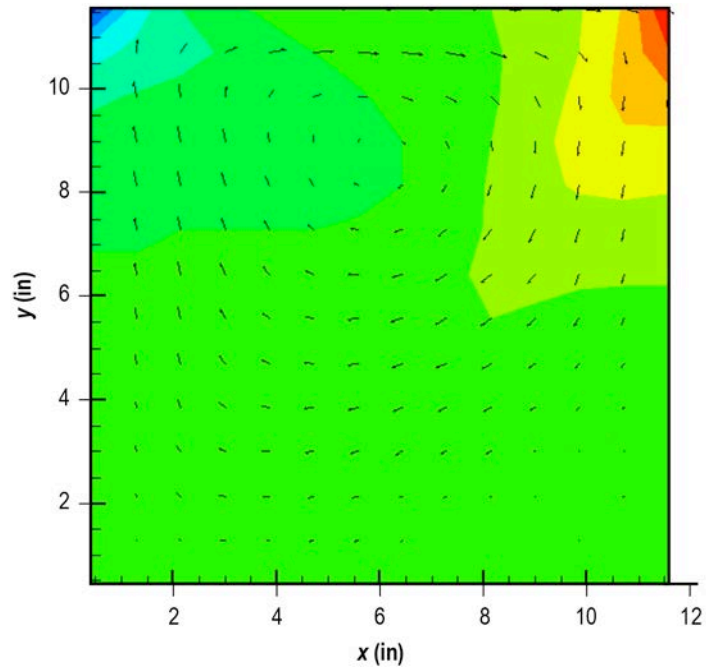


Figure 7. Predicted velocity field and pressure contours.

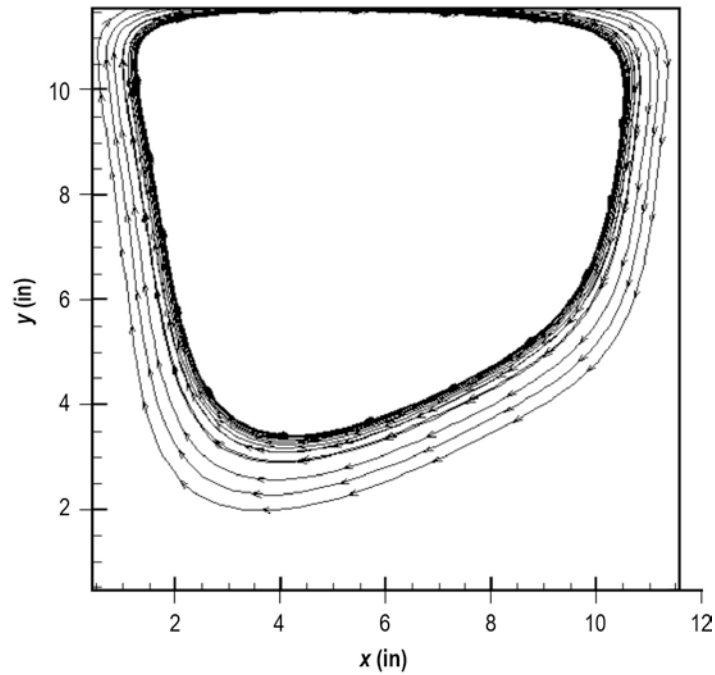


Figure 8. Predicted stream traces in the driven cavity.

B. Fluid Transient

This example deals with water hammer in a pipe with entrapped air. GFSSP results are validated against experimental data available in the literature.¹⁴ A 1.025-in-diameter long pipe is attached to a reservoir of water at one end and closed at the other end with some entrapped air. A ball valve separates the water from the air as shown in Fig. 9. The ball valve is closed until about 0.15 s, and then gradually opens to 100% at about 0.4 s. This example has been set up according to the experimental study done by Lee and Martin.¹⁴ The two most important controlling parameters for this problem are the reservoir pressure (p_R) and the fractional air length present in the pipe as compared to the total pipe length ($\alpha_g = L_g/L_T$). The initial length for the water volume in the pipe (L_l) is fixed to 20 ft, and the initial length of the air column in the pipe (L_g) varies from a low of 1.23 ft to 16.23 ft, the value of α ranging from 0.0579 to 0.448, respectively. The ratio of reservoir pressure to the initial pressure of the entrapped air ($P_R = p_R/p_{\text{atm}}$) varies in the range of 2 to 7, i.e., the reservoir pressure (p_R) range being 29.4 psi to 102.9 psi. The objective of this study is to predict the transient pressure at different points along the length of the pipe.

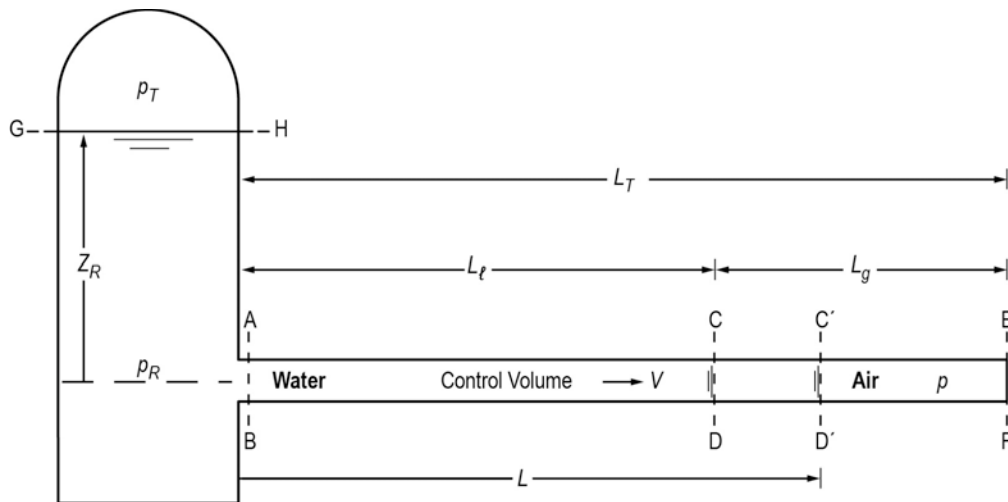


Figure 9. Schematic of the water pipe with entrapped air.

The GFSSP model to represent the flow of water in the pipe is shown in Fig. 10. The 20-ft-long pipe sector (only the water column) is divided into 10 uniform pipe segments and one restriction separating 12 nodes. Boundary node 1 represents the tank (reservoir). A User Subroutine interfaces node 12 to an unseen pseudo control volume containing air only. The pseudo control volume has a fixed mass of air, but the volume changes as it is pressurized, owing to the fluctuation of pressure at node 12. Thereby, the volume of node 12 changes as the volume of the imaginary control volume changes. The volume change in node 12 is computed by a volume balance between the volume of water and the volume of the entrapped air. The total volume ($V_{tot} = V_{air} + V_{12}$) remains constant, and must be equal to the initial total volume (since the pipe is closed at the other end).

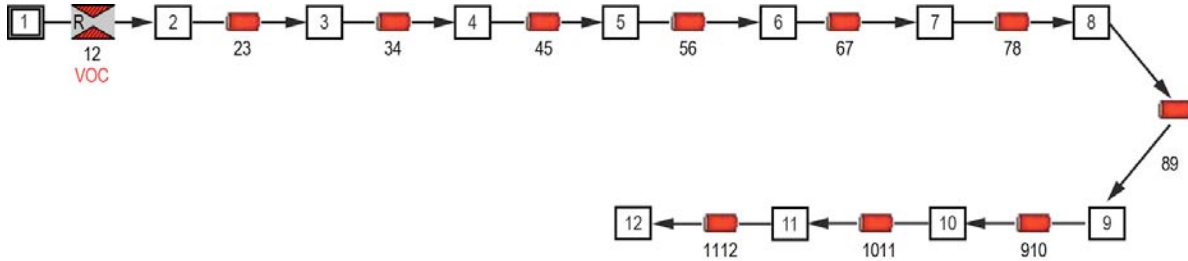


Figure 10. GFSSP model of sudden valve opening experiment of Lee and Martin.¹⁴

For the numerical solution a time step of 0.01 s has been used. The operating conditions are: $P_R = 7$ and $\alpha_g = 0.45$. Figure 11 compares GFSSP's predicted pressure at node 12 with that of the experimental data points of Lee and Martin. The predicted results compared very well, and even though the peak pressure amplitude differs by about 7%, the frequencies of pressure oscillations matched very well.

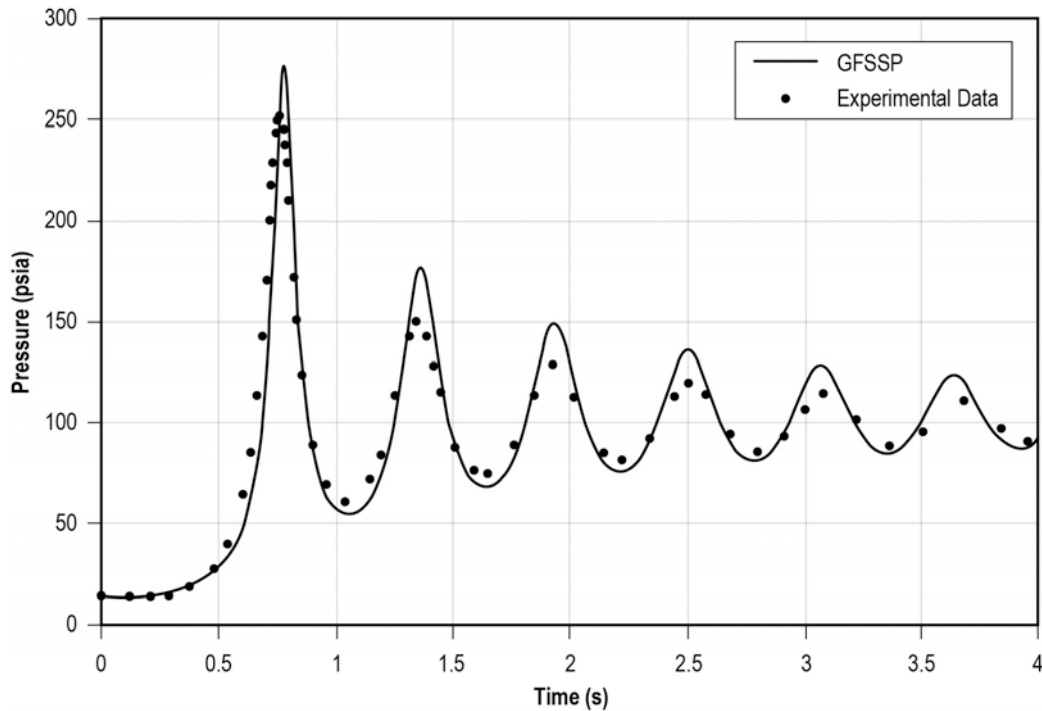


Figure 11. Comparison of GFSSP and experimental data.

A Fast Fourier Transform (Fig. 12) has been conducted in the numerical model to predict the different modal frequencies of the pressure transient and also compared with the experimental data. More details of this example problem are available in Ref. 15.

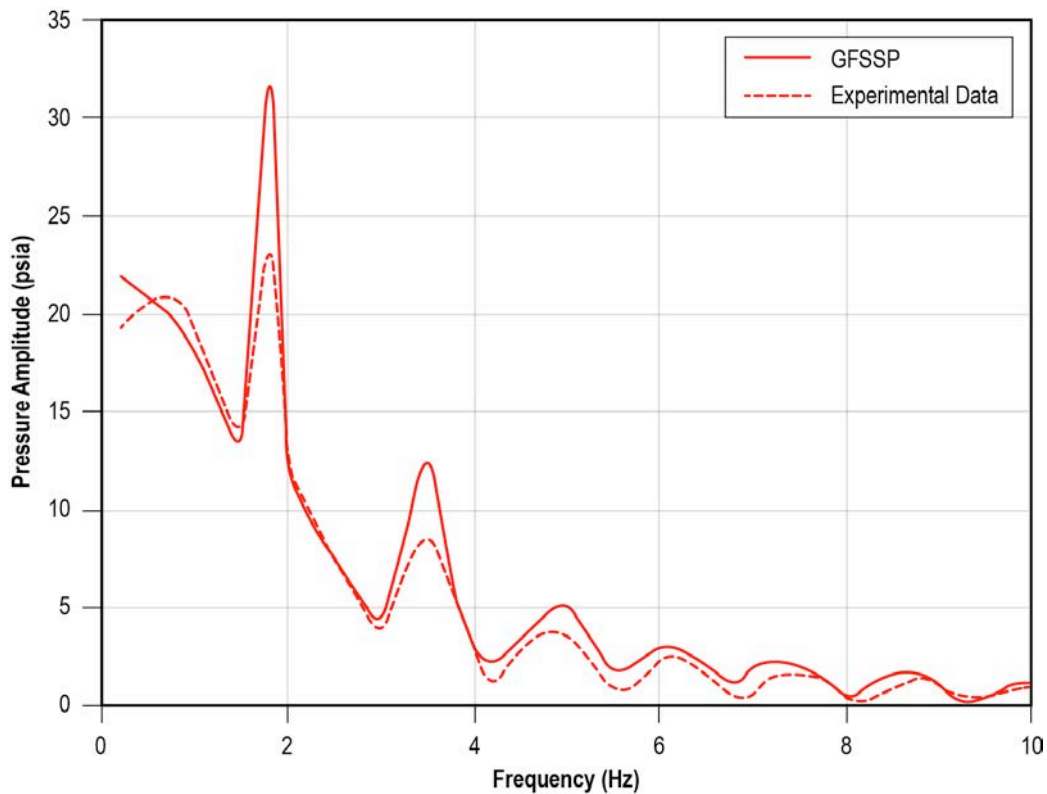


Figure 12. Fast Fourier Transform for modal frequencies.

C. Chilloidn of Cryogenic Transfer Line

For this example, the chilloidn of cryogenic pipeline to validate GFSSP’s transient conjugate heat transfer capability has been selected. In the 1960s, the National Bureau of Standards (NBS) conducted a series of chilloidn experiments on a cryogenic transfer line.¹⁶ The test setup (Fig. 13) is a vacuum-jacketed, 200-ft-long copper pipe of 5/8-in inner diameter. A pressurized 80-gal dewar feeds liquid hydrogen (LH₂) into the pipe that is initially at ambient temperature. The wall temperature is measured at four thermocouple stations at distances of 20, 80, 141, and 198 feet from the inlet.

When the fluid touches the relatively warm pipe walls, heat transfer causes the liquid cryogen to boil and the pipe wall temperature to decrease. Eventually, the pipe chills down to the liquid temperature, and the liquid front gradually travels further down the pipeline. At the outlet of the pipeline, vapor exits to the atmosphere.

The NBS experiments were conducted with LH₂ and liquid nitrogen (LN₂) at various driving pressures with saturated and subcooled fluid. This example problem models one of the tests with an inlet boundary of saturated LH₂ at 74.97 psia and -411 °F.

Figure 14 shows the GFSSP model of the chilloidn experiment. The pipeline has been discretized into 30 pipe branches, each 80 in long. There are 31 fluid nodes, and each fluid node is connected with solid nodes. The total mass is distributed to 31 solid nodes. The fluid and solid nodes are connected by solid-to-fluid conductors. The solid nodes are connected by solid-to-solid conductors. The boundary nodes 1 and 33 represent the inlet dewar and ambient outlet, respectively.

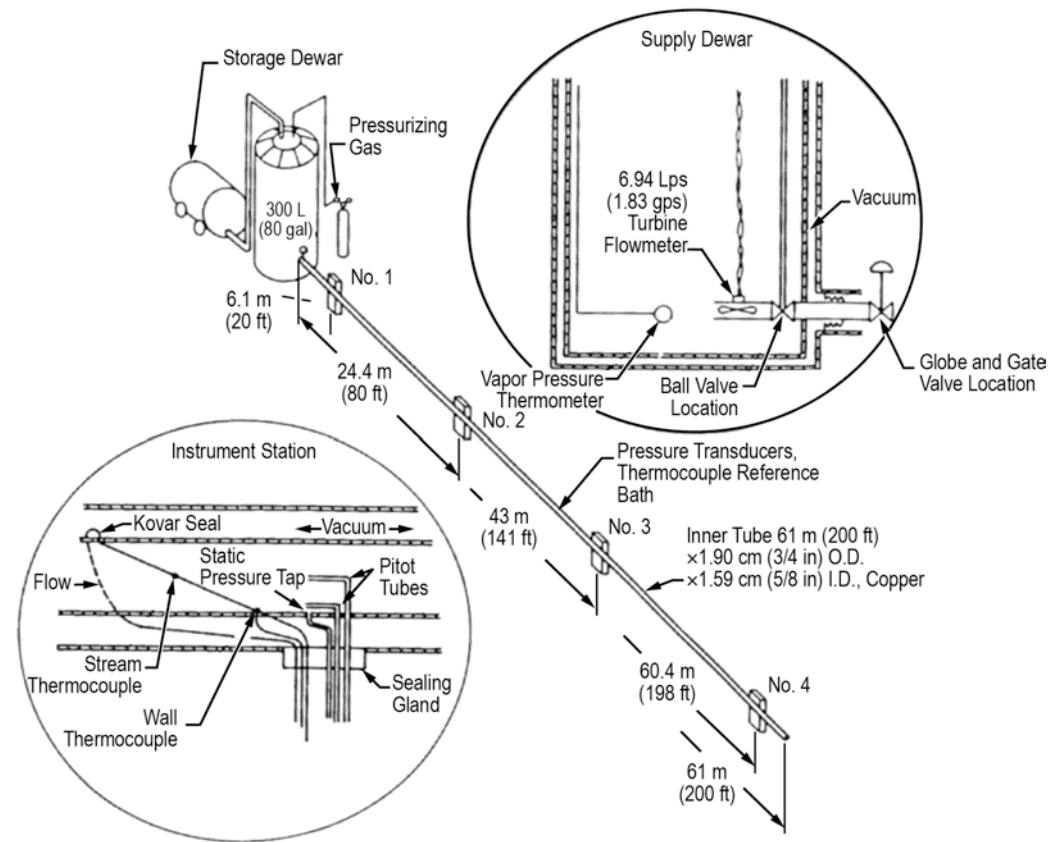


Figure 13. NBS test setup of cryogenic transfer line.

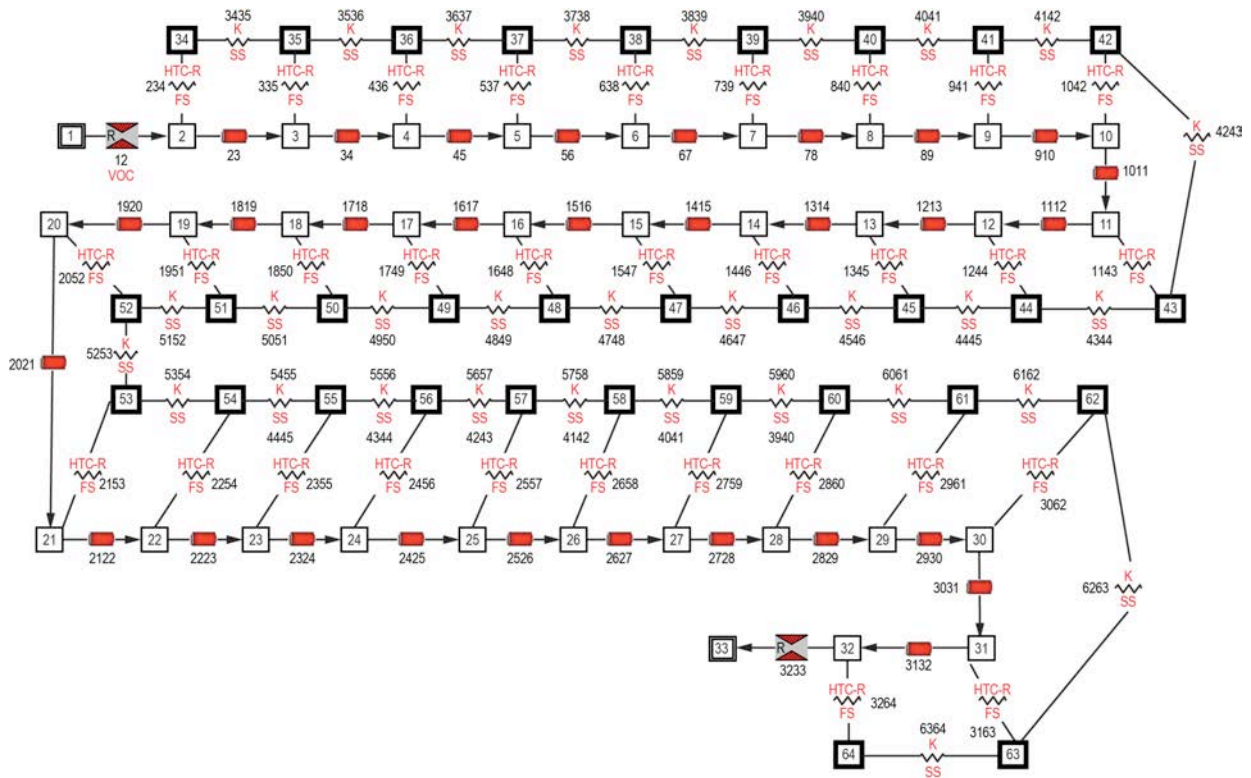


Figure 14. GFSSP model of the cryogenic pipeline.

The solid nodes are connected to the fluid nodes by fluid-to-solid conductors, which model convection from the fluid to the pipe wall. The built-in Miropolskii correlation¹⁷ is used to calculate the convection coefficient for the two-phase flow. Because the pipe is vacuum-jacketed, heat transfer between the pipe walls and the ambient is assumed negligible.

Figure 15 shows the comparison between predicted and measured temperatures at four measuring stations. The predictions and measurements compare reasonably well. In general, measurements show more rapid chilldown than did the predictions. This discrepancy can be attributed to the deficiency of heat transfer correlation that does not account for other boiling regimes such as nucleate and transition.

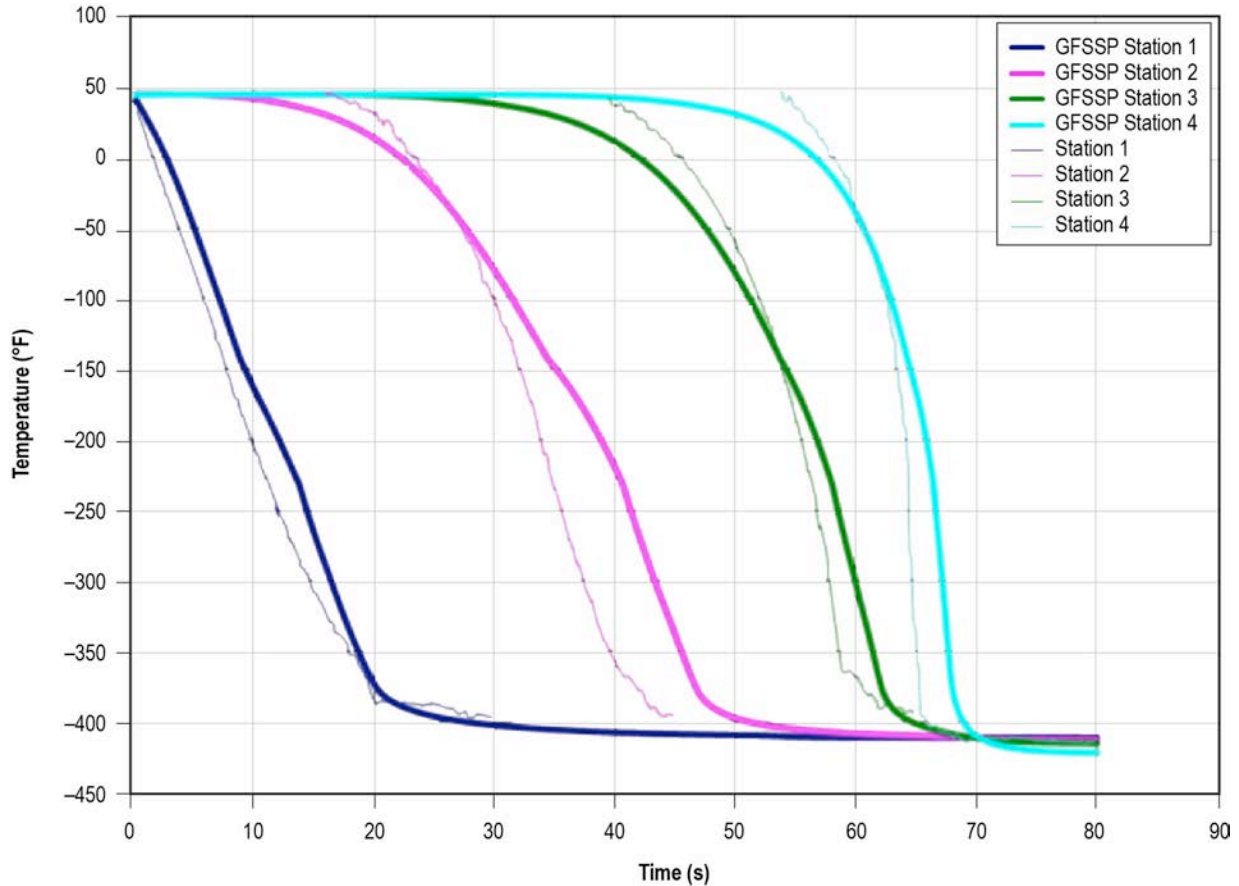


Figure 15. GFSSP’s predicted solid temperatures (°F) compared to measurements.

The comparison of measured and predicted chilldown time of the transfer line at different driving pressures for both LH₂ and LN₂ is shown in Table 6. Chilldown time decreases with increasing pressure primarily due to a higher flow rate at higher pressure. Subcooling helps reduce chilldown time. Generally, predicted chilldown time is slightly higher than measured data. Discrepancy between the predictions and measurements can be attributed to the inaccuracy in the heat transfer coefficient correlation as discussed previously. More details about this validation appear in Ref. 18.

Table 6. Measured and predicted chilldown time for NBS test setup.

Saturated LH₂ chilldown time for various driving pressures

Driving Pressure (psia)	Saturation Temperature (°F)	Experimental Chilldown Time (s)	Predicted Chilldown Time (s)
74.97	-411.06	68	70
86.73	-409.08	62	69
111.72	-406.4	42	50
161.72	-402.13	30	33

Subcooled LH₂ chilldown time for various driving pressures. LH₂ is subcooled at -424.57 °F

Driving Pressure (psia)	Experimental Chilldown Time (s)	Predicted Chilldown Time (s)
36.75	148	150
61.74	75	80
86.73	62	60
111.72	41	45
136.72	32	35
161.7	28	30

Saturated LN₂ chilldown time for various driving pressures

Driving Pressure (psia)	Saturation Temperature (°F)	Experimental Chilldown Time (s)	Predicted Chilldown Time (s)
61.74	-294.09	165	185
74.97	-289.71	150	160
86.73	-286.24	130	140

Subcooled LN₂ chilldown time for various driving pressures. LN₂ is subcooled at -322.87 °F

Driving Pressure (psia)	Experimental Chilldown Time (s)	Predicted Chilldown Time (s)
36.75	222	250
49.97	170	175
61.74	129	140
74.97	100	100
86.73	85	90

D. Self-Pressurization of Cryogenic Tank

The purpose of this example is to demonstrate the simulation of self-pressurization of an LH₂ tank performed under the Multipurpose Hydrogen Test Bed (MHTB) program.¹⁹ The purpose of the MHTB program is to test a thermodynamic vent system (TVS) to reduce boil-off in a cryogenic propellant tank for long-term storage of propellant in space, as shown schematically in Fig. 16.

The MHTB 5083 aluminum tank is cylindrical in shape with a height and diameter of 10 ft and elliptic domes in both ends, as shown in Fig. 17. It has an internal volume of 639 ft³ and surface area of 379 ft². Initially, the tank is allowed to self-pressurize due to boil-off and by not allowing the vapor to vent. Once the pressure reaches the maximum allowable pressure, LH₂ is introduced into the tank through the spray bar. The pressure begins to fall due to heat transfer, and when the pressure reaches the minimum allowable pressure, the spray is stopped and the tank is allowed to self-pressurize; thus, the TVS cycle continues. The purpose of the GFSSP model is to simulate the initial self-pressurization when ullage pressure rises from the initial tank pressure to the upper bound pressure when the spray starts. The GFSSP model results were then compared with the test data. A 50% fill level case was modeled to simulate the self-pressurization test.

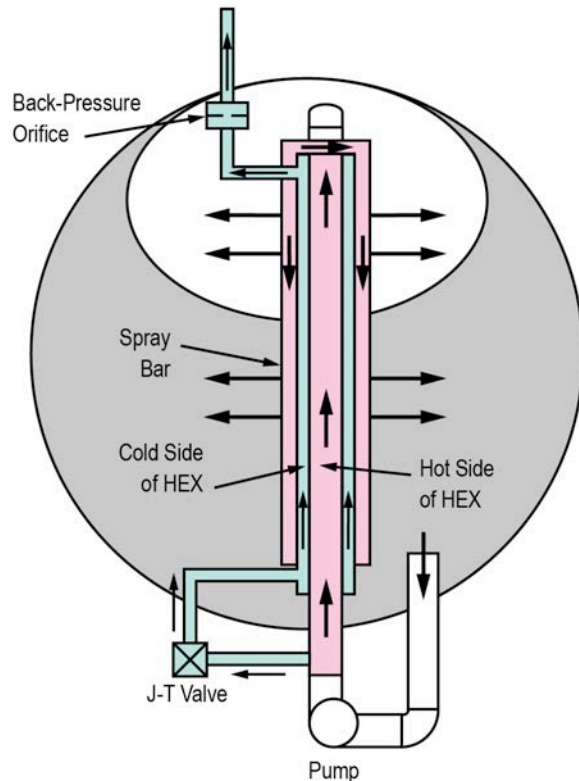


Figure 16. TVS in MHTB tank.

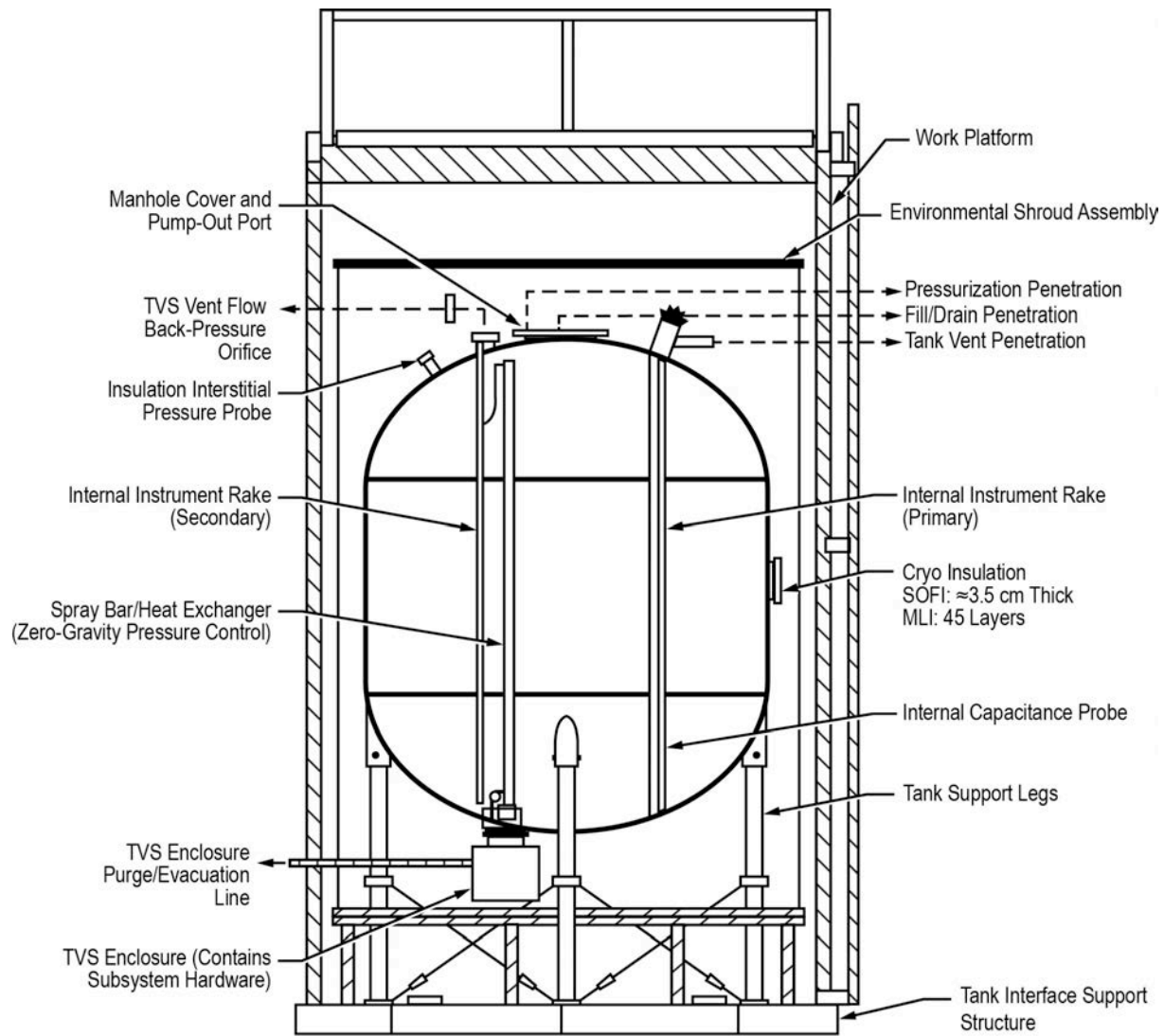


Figure 17. MHTB test tank and supporting hardware schematic.

Figure 18 shows the GFSSP model of self-pressurization in the MHTB tank at the 50% fill level. Node 4 represents LH₂; nodes 2, 8, 9, 10, and 11 represent the ullage at different fill levels. Node 3 is a pseudo boundary node separating LH₂ from vapor hydrogen in the ullage space. Branches 45, 164, 162, 168, 169, 1610, and 1611 are for introducing LH₂ into the tank through the TVS spray bar. These branches are inactive during self-pressurization of the tank. Nodes 7, 6, 12, 13, 14, and 15 are solid nodes representing the aluminum tank wall. Solid node 7 is connected with LH₂ stored in fluid node 4. In this model, heat leak through insulation is calculated in the User Subroutine and applied in the solid nodes as a source term.

In this model, a User Subroutine was used to (1) model evaporative mass transfer at the liquid-vapor interface, (2) calculate the heat transfer coefficient between the wall and the fluid nodes, and (3) calculate heat transfer through the multilayer insulation (MLI) blankets. The details of the modeling appear in Ref. 20.

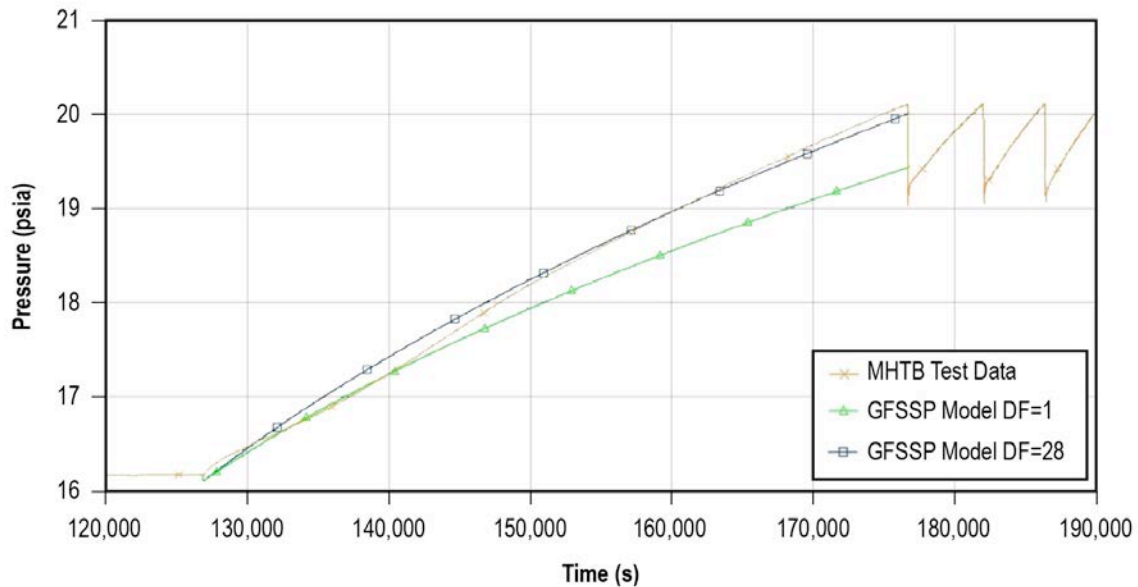


Figure 19. Application results for MHTB self-pressurization model.

E. No-Vent Chill and Fill of Cryogenic Tank

The purpose of this example is to demonstrate the simulation of the no-vent chill and fill method of chilling and filling a cryogenic tank. The practice of tank chilldown in a microgravity environment is quite different than tank chilldown on the ground. On the ground, under normal gravity, a vent valve on top of the tank can be kept open to vent the vapor generated during the chilling process. The tank pressure can be kept close to atmospheric pressure while the tank is chilling down. In a microgravity environment, due to the absence of stratification, such a practice may result in dumping a large amount of precious propellant overboard. The intent of the no-vent chill and fill method is to minimize the loss of propellant during chilldown of a propellant tank in a microgravity environment. The no-vent chill and fill method consists of a repeated cyclic process of charge, hold, and vent.

During the charge cycle, a small quantity of liquid cryogen is injected into the evacuated tank. Some type of spray nozzle is usually used to break the incoming liquid into droplets. Initially, the liquid flashes due to the low tank pressure, and then the remaining liquid droplets evaporate as they contact warm hydrogen vapor or the tank wall. During the hold period, the circulating flow pattern induced from the spray nozzles provides convective heat transfer from cold vapor to the tank wall. The primary mode of heat transfer during the hold is convection. At the completion of the hold period, the pressure has risen considerably and the tank is ready to be vented. Since venting occurs as an isentropic blowdown, some additional cooling may be recovered with stage-wise venting. The key parameters of this method are (1) charge magnitude, (2) spray system selection, (3) mass flow rate, (4) hold duration, (5) acceleration environment, (6) desired tank wall temperature, and (7) maximum operating pressure. A reliable and inexpensive mathematical model will help designers to perform a large amount of calculations to optimize the key parameters. A GFSSP model was developed to simulate chilldown of the LH₂ tank at the K-site Test Facility²¹ and numerical predictions were compared with test data.

The test setup at the K-site Test Facility, shown in Fig. 20, consists of a test tank, spray system, test tank valves, instrumentation, and the vacuum chamber.

The test tank selected was ellipsoidal with an 87-in major diameter and a 1.2 to 1 major to minor axis ratio. The two ends are joined by a short 1.5-in cylindrical section. The tank is made of 2219 aluminum chemically milled to a nominal thickness of 0.087 in. Thicker sections exist where they were required for manufacturing (mainly weld lands). The tank has a 28.35-in access flange on the top, weighs 329.25 lb, and has a volume of 175 ft³. The tank was originally designed for a maximum operating pressure of 80 psia. Prior to the start of testing, the tank was requalified by pneumatic test for a maximum operating pressure of 50 psia. The tank is covered with a blanket of 34 layers of MLI made with double-aluminized Mylar and silk net spacers, and is supported by 12 fiberglass epoxy struts. The test environment ambient temperature was uniform and maintained at 530R ± 1R by an electrically heated shroud located outside the tank and inside the vacuum chamber.

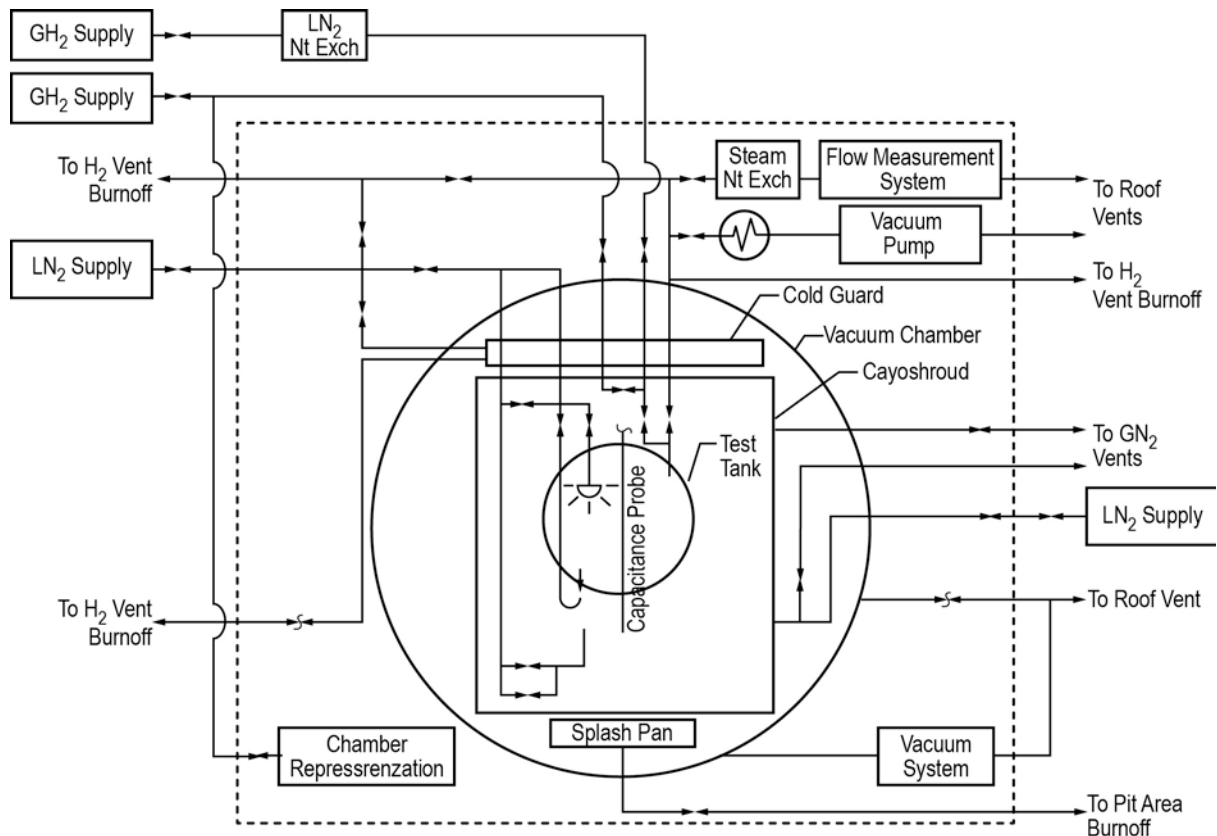


Figure 20. K-site test setup for no-vent fill experiment.

A nine-node tank model (Fig. 21) was developed to model this experiment. The tank was discretized into nine nodes and eight branches. Each fluid node was connected to a corresponding solid node. The total flow rate was equally distributed into nine branches with the fixed flow rate option.

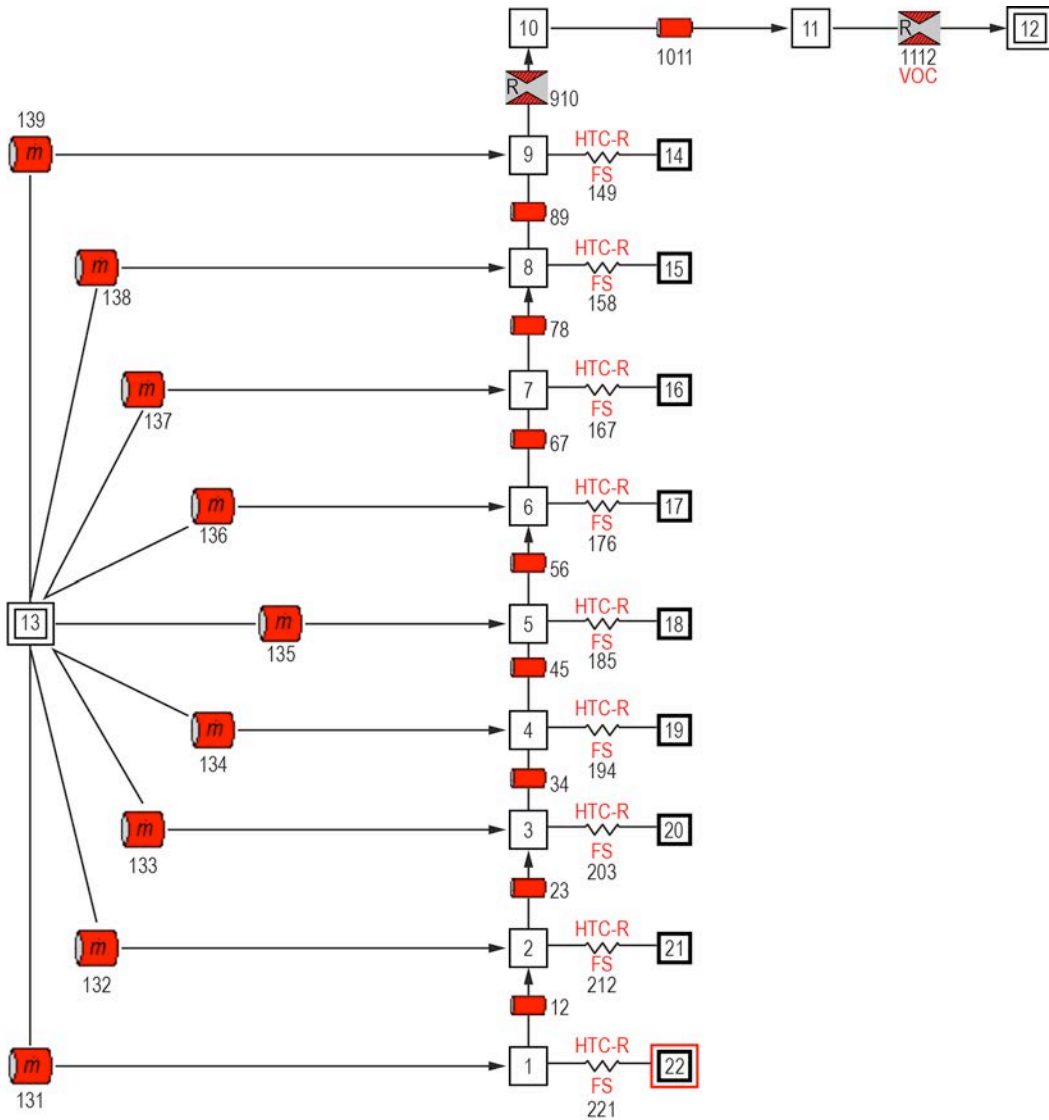


Figure 21. GFSSP nine-node tank model.

Inlet flow rate into the tank and predicted pressure are shown in Fig. 22. There are five short pulses of LH₂ flow into the tank. After each pulse, there is a period of no flow into the tank. During this period, the tank holds the propellant with the vent valve closed for the tank to reach thermal equilibrium with cold vapor. Pressure rises almost instantaneously because of the liquid turning into vapor with a large increase in specific volume. The pressure continues to increase at a lower rate due to heat transfer from the wall during this hold period. The hold period is followed by venting, causing pressure to drop rapidly. After shutting the vent valve, the next pulse of inlet flow occurs. After five pulses, a constant inlet flow was maintained to fill the tank. Once the continuous filling starts, pressure initially drops due to some condensation of vapor in the tank. Once the tank is nearly filled, pressure rises due to the compression of vapor in the ullage space.

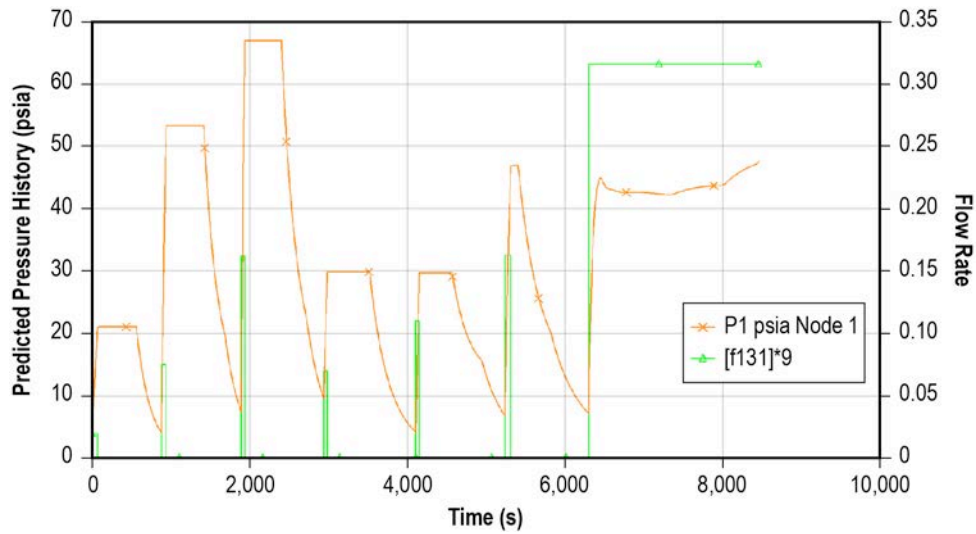


Figure 22. Specified inlet flow rate (green) and predicted pressure (orange) history.

Figure 23 shows the predicted mass history of hydrogen during the operation. There is very little hydrogen during the chilling process because of venting. The total amount of propellant vapor vented during this period is 32.5 lb. This number compares well (within 1.5%) with measured propellant loss during the test.

Temperatures were measured during the test. The upper and lower bound measured temperature history is shown in Fig. 24. GFSSP model results for single-node and nine-node tank temperatures are also shown to compare the predicted and measured test data. For the nine-node model, the centerline temperature is plotted.

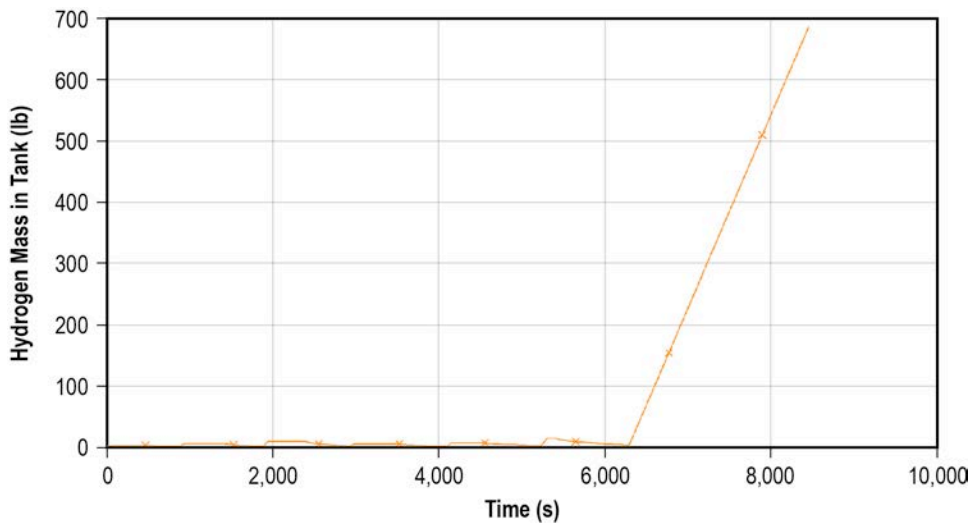


Figure 23. Predicted hydrogen mass history in the tank.

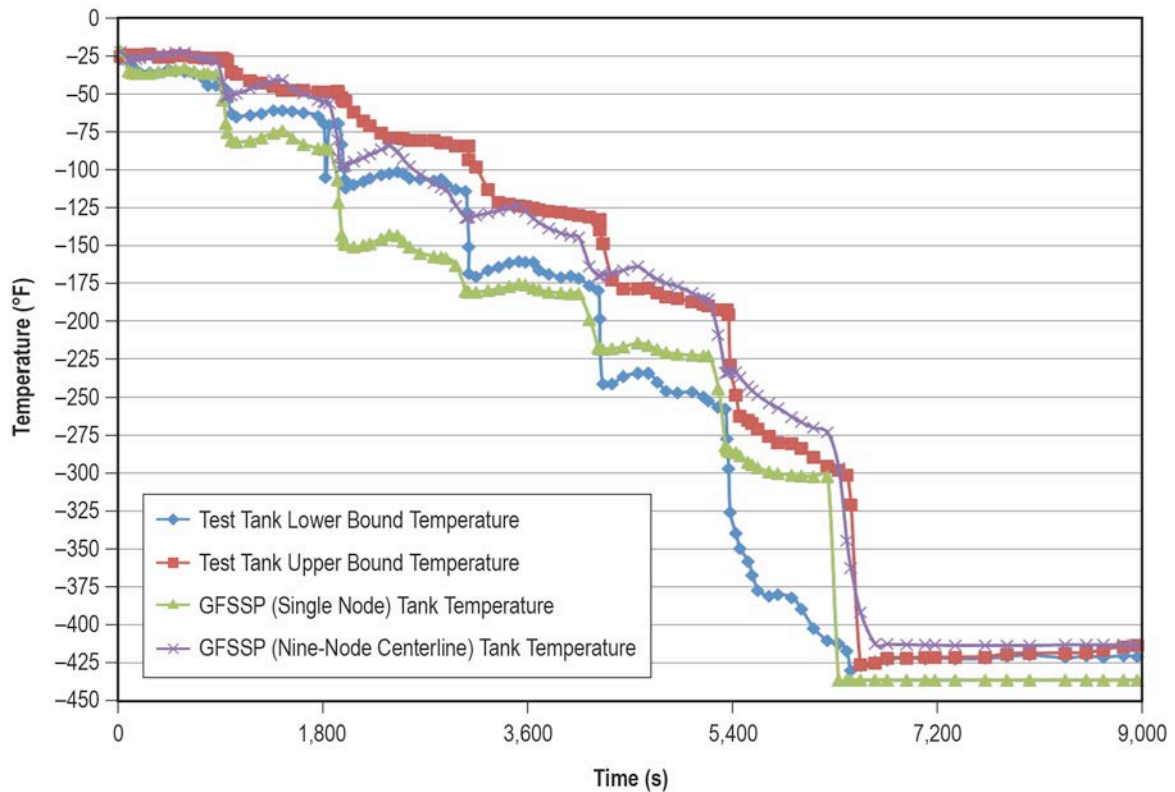


Figure 24. Comparison of predicted and measured wall temperature during no-vent fill for the K-site test tank.

V. Conclusions

This paper explains the basic features of NASA’s Generalized Fluid System Simulation Program (GFSSP) and describes the additional capabilities of version 6. Several numerical models are presented to illustrate code’s application in simulating fluid transient and cryogenic fluid management applications such as chilldown of the cryogenic transfer line, no-vent chill and fill of the cryogenic tank, and self-pressurization of the cryogenic tank. Numerical results are compared with test data.

Acknowledgments

GFSSP development was supported by the National Institute of Rocket Propulsion at Marshall Space Flight Center (MSFC), the Launch Service Program at Kennedy Space Center, and the Evolvable Cryogenics Project at NASA’s Glenn Research Center. The authors wish to acknowledge the services of the Technology Transfer Office for distribution of the GFSSP and the STI Publications Office at MSFC for the preparation of this manuscript.

References

- ¹Streeter, V. L., *Fluid Mechanics*, 3rd ed., McGraw-Hill, New York, 1962.
- ²SINDA/G Thermal Analyzer, Network Analysis Inc., URL: <http://www.sinda.com> [cited January 2001].
- ³SINDA/FLUINT, Heat Transfer and Fluid Flow Design and Analysis Software, C&R Technologies, URL: <http://www.crtech.com/sinda.html> [cited January 2001].
- ⁴Majumdar, A. K., LeClair, A. C., Moore, R., and Schallhorn, P. A., "Generalized Fluid System Simulation Program, Version 6.0," NASA/TM—2013–217492, Oct. 2013.
- ⁵Patankar, S. V., *Numerical Heat Transfer and Fluid Flow*, Hemisphere Publishing Corp., Washington, DC, 1980.
- ⁶Hendricks, R. C., Baron, A. K., and Peller, I. C., "GASP—A Computer Code for Calculating the Thermodynamic and Transport Properties for Ten Fluids: Parahydrogen, Helium, Neon, Methane, Nitrogen, Carbon Monoxide, Oxygen, Fluorine, Argon, and Carbon Dioxide," NASA TN D-7808, Feb. 1975.
- ⁷Hendricks, R. C., Peller, I. C., and Baron, A. K., "WASP - A Flexible Fortran IV Computer Code for Calculating Water and Steam Properties," NASA TN D-7391, Nov. 1973.
- ⁸*User's Guide to GASPAK, Version 3.20*, Cryodata, Inc., Nov. 1994.
- ⁹*Winplot Version 4.3 User's Manual*, NASA Marshall Space Flight Center, Huntsville, AL, 2008.
- ¹⁰Lemmon, E. W., Huber, M. L., and McLinden, M. O., "NIST Reference Fluid Thermodynamic and Transport Properties—REFPROP, Version 8.0, User's Guide," URL: <http://www.nist.gov/srd/upload/REFPROP8.PDF> [cited April 2007].
- ¹¹Schallhorn, P. A., and Hass, N., "Forward Looking Pressure Regulator Algorithm for Improved Modeling Performance Within the Generalized Fluid System Simulation Program," *40th AIAA/ASME/SAE/ASEE Joint Propulsion Conference and Exhibit*, AIAA 2004-3667, AIAA, Reston, VA, 2004.
- ¹²Schallhorn, P. A., and Majumdar, A. K., "Implementation of Finite Volume Based Navier Stokes Algorithm Within General Purpose Flow Network Code," *50th AIAA Aerospace Sciences Meeting*, AIAA 2012-1149, AIAA, Reston, VA, 2012.
- ¹³Burggraf, O. R., "Analytical and Numerical Studies of the Structure of Steady Separated Flows," *Journal of Fluid Mechanics*, Vol. 24, Part 1, 1966, pp. 113-151.
- ¹⁴Lee, N. H., and Martin, C. S., "Experimental and analytical investigation of entrapped air in a horizontal pipe," *Proceedings of the 3rd ASME/JSME Joint Fluids Engineering Conference*, ASME, New York, 1999, pp. 1-8.
- ¹⁵Bandyopadhyay, A., and Majumdar, A. K., "Network Flow Simulation of Fluid Transients in Rocket Propulsion System," *Journal of Propulsion and Power*, Vol. 30, No. 6, Oct. 2014.
- ¹⁶Brennan, J. A., Brentari, E. G., Smith, R. V., and Steward, W. G., "Cooldown of Cryogenic Transfer Lines, An Experimental Report," Report 9264, National Bureau of Standards, 1966.
- ¹⁷Cross, M., Majumdar, A. K., Bennett, J., and Malla, R., "Modeling of Chill Down in Cryogenic Transfer Lines," *Journal of Spacecraft and Rockets*, Vol. 39, No. 2, 2002, pp. 284-289.
- ¹⁸Majumdar, A. K., and Ravindran, S. S., "Numerical Modeling of Conjugate Heat Transfer in Fluid Network," *Journal of Propulsion and Power*, Vol. 27, No. 3, 2011, pp. 620-630.
- ¹⁹Martin, J. J., and Hastings, L. J., "Large-Scale Liquid Hydrogen Testing of a Variable Density Multilayer Insulation With a Foam Substrate," NASA/TM—2001–211089, June 2001.
- ²⁰Majumdar, A. K., Valenzuela, J., LeClair, A., and Moder, J., "Numerical Modeling of Self-Pressurization and Pressure Control by Thermodynamic Vent System in a Cryogenic Tank," *26th Space Cryogenics Workshop*, Cryogenic Society of America, Inc., Oak Park, IL (to be published).
- ²¹Chato, D. J., and Sanabria, R., "Review and Test of Chillydown Methods for Space-Based Cryogenic Tanks," NASA Technical Memorandum 104458, AIAA-91-1843, *27th AIAA/ASME/SAE/ASEE Joint Propulsion Conference*, NASA, Cleveland, OH, 1991.